

Seasonal Influence of the Quasi-Biennial Oscillation on Stratospheric Jets and Rossby Wave Breaking

MATTHEW H. HITCHMAN AND AMIHAN S. HUESMANN*

Department of Atmospheric Sciences, University of Wisconsin—Madison, Madison, Wisconsin

(Manuscript received 30 September 2007, in final form 20 July 2008)

ABSTRACT

The influence of the stratospheric quasi-biennial oscillation (QBO) on the polar night jets (PNJs), subtropical easterly jets (SEJs), and associated Rossby wave breaking (RWB) is investigated using global meteorological analyses spanning 10 recent QBO cycles. The seasonal dependence of the descent of the QBO is shown by using five layered shear indices. It is found that the influence of the QBO is distinctive for each combination of QBO phase, season, and hemisphere (NH or SH). The following QBO westerly (W) minus easterly (E) differences in the PNJs were found to be significant at the 97% level: When a QBO W (E) maximum is in the lower stratosphere (~ 500 K or ~ 50 hPa), the NH winter PNJ is stronger (weaker), in agreement with previous results (mode A). Mode A does not appear to operate in other seasons in the NH besides DJF or in the SH in any season. When a QBO W (E) maximum is in the middle stratosphere (~ 700 – 800 K or ~ 10 – 20 hPa), the PNJ in the SH spring is stronger (weaker), also in agreement with previous results (mode B). It is found that mode B also operates in the NH spring. A third distinctive mode is found during autumn in both hemispheres: a QBO W (E) maximum in the middle stratosphere coincides with a weaker (stronger) PNJ (mode C). The signs of wind anomalies are the same at low and high latitudes for modes A and B, but are opposite for mode C. This sensitive dependence on QBO phase and season is consistent with the nonlinear nature of the interaction between planetary waves and the shape of the seasonal wind structures.

During the solstices the meridional circulation associated with QBO connects primarily with the winter hemisphere, whereas during the equinoxes it is more symmetric about the equator. QBO W enhance the equatorial potential vorticity (PV) gradient maximum, but the time-mean maximum may be related to chronic instabilities in the subtropics. The equatorial PV gradient maximum and flanking RWB tend to be more pronounced in the Eastern Hemisphere in stratospheric analyses.

When QBO W are in the middle stratosphere, the flanking PV gradient minima (SEJs) are enhanced and RWB is more frequent and symmetric about the equator. When QBO W are in the upper stratosphere, a strong seasonal asymmetry is seen, with enhanced RWB in the summer SEJ, primarily during boreal winter. This is consistent with an upward increase of summer to winter flow and modulation by a strong “first” and weak “second” semiannual oscillation.

1. Introduction

The stratospheric quasi-biennial oscillation (QBO; Reed et al. 1961; Wallace 1973; Baldwin et al. 2001), with its irregular (22–32 months) periodic reversal in zonal wind, creates long-lasting anomalies that influence the globe. In 1980, Holton and Tan (1980) dis-

covered a significant correlation between QBO westerlies (W) at 50 hPa and the strength of the boreal polar night jet (PNJ). They suggested that sudden stratospheric warmings are less likely during QBO W, when the zero wind line lies in the summer subtropics. The QBO modulates the position of critical surfaces and thus the propagation and absorption of extratropical planetary Rossby waves (e.g., Holton and Austin 1991; Haynes et al. 1991; O’Sullivan and Young 1992; O’Sullivan and Chen 1996; Kinnersley and Pawson 1996; Hamilton 1998; Niwano and Takahashi 1998; Gray et al. 2001). When QBO easterlies (E) are in the tropical stratosphere, the zero wind line lies in the winter subtropics, and planetary Rossby wave breaking (RWB) is more likely to occur in the northern winter

*Current affiliation: Gustavus Adolphus College, St. Peter, Minnesota.

Corresponding author address: Matthew H. Hitchman, Department of Atmospheric and Oceanic Sciences, University of Wisconsin—Madison, 1225 W. Dayton St., Madison, WI 53706.
E-mail: matt@aos.wisc.edu

(McIntyre and Palmer 1983). This takes the form of a large occlusion, with a surge of warm air over the pole causing a sudden warming. During QBO W, wave activity extends over a larger volume; hence, RWB is less likely and the PNJ tends to be stronger. Some of these studies emphasized the sensitivity of the influence of the QBO to the vertical location of QBO wind anomalies, a theme which is explored further in this paper.

Another significant statistical relationship was found by Newman and Randel (1988) and Baldwin and Dunkerton (1998): during SH spring the PNJ is stronger when QBO W are in the middle stratosphere. Naito et al. (2003) diagnosed QBO influences in perpetual winter simulations of ~ 27 yr duration, with either QBO E or W winds maximizing near 50 hPa. They found polar temperatures to be systematically warmer during QBO E and found significant influences in the troposphere. This paper describes the relationship between the QBO and the PNJs for each season, hemisphere, and phase of the QBO, averaged over 10 cycles.

Further motivation for exploring this relationship comes from the known influence of the QBO on the distribution of ozone (Hasebe 1983; Shiotani 1992; Randel and Cobb 1994; Kinnarsley and Tung 1998), volcanic aerosol (Trepte and Hitchman 1992; Hitchman et al. 1994), and other radiatively and chemically important trace constituents. Moreover, the QBO can influence tropospheric weather via vertical coupling in the extratropics (Baldwin and Dunkerton 2001; Thompson and Wallace 2001; Wallace and Thompson 2002; Robinson 2000; Thompson and Solomon 2002; Thompson et al. 2005) or by modulating deep convection in the tropics (Reid and Gage 1985; Gray et al. 1990; Collimore et al. 1998; Giorgetta et al. 1999; Collimore et al. 2003). In this work we employ global meteorological analyses after 1978 and calculate RWB statistics to further explore the relationship between the QBO, waves, and wind structure.

A reversed potential vorticity (PV) gradient can indicate the presence of an amplifying Rossby wave, causing differential advection of PV contours to the point of PV gradient reversal, or RWB (McIntyre and Palmer 1983). A reversed gradient implies 3D folding of material contours, an enstrophy cascade, and ensuing mixing; hence, the distribution of RWB is a useful indicator of irreversible transport by synoptic- and planetary-scale Rossby waves. RWB statistics have been calculated for various locations and seasons by Baldwin and Holton (1988), Peters and Waugh (1996, 2003), Postel and Hitchman (1999, 2001), Waugh and Polvani (2000), Knox and Harvey (2005), Berrisford et al. (2007), and Martius et al. (2007). Hitchman and Huesmann (2007, hereafter HH07) provided a seasonal climatology of RWB statis-

tics throughout the 330–2000-K layer. HH07 showed a striking structure at the equator: a strong PV gradient occurs in each season, flanked by RWB in the subtropics, primarily on the summer side. This paper explores the influence of the QBO on the distribution of RWB statistics, including the PV gradient, which describes jet structure, and the frequency and strength of reversals. Focal topics include the QBO influence on the equatorial PV gradient maximum, PNJs, subtropical easterly jets (SEJs), and the associated RWB.

Haynes and Shuckburgh (2000a,b) used the coordinate transformation technique of Nakamura (1996) to create a climatology of effective diffusivity, which exhibits similar patterns to the RWB distributions of HH07. Shuckburgh et al. (2001) used 6 yr of European Centre for Medium-Range Weather Forecasts (ECMWF) data in the 380–800-K layer to show that QBO W enhance barotropic instability waves in the SEJ, with characteristic zonal wavenumbers 6–10. This zonal scale is also visible in Fig. 6e of HH07. With increasing altitude, one expects an increase in growing and breaking synoptic Rossby waves in the SEJs (Salby 1981; Plumb 1983; Burkes and Leovy 1986; Limpasuvan and Leovy 1995; Orsolini et al. 1997; Shuckburgh et al. 2001). Shuckburgh et al. (2001) showed that the PV gradient is reversed and EP fluxes are divergent on both flanks of QBO W.

Planetary waves entering the tropical middle atmosphere from a westerly hemisphere can trigger inertial instability (Hitchman et al. 1987). Strong negatively curved zonal flow at the equator is compatible with strong inertial instability on the winter side and with a more strongly positively curved SEJ and greater barotropic instability on the summer side (Hitchman 1985). This would tend to favor RWB on the summer side during QBO W, with the effect increasing into the upper stratosphere. A discussion of inertial instability and the summer to winter flow is given by Semeniuk and Shepherd (2001).

The goals of this paper are to explore the influence of the QBO on the structure of stratospheric jets and RWB for each season in both the SH and NH. Section 2 describes the data and analysis methods. In section 3 the effect of the QBO on the equatorial PV gradient maximum is explored. In section 4 the seasonal dependence of the meridional structure of the QBO is explored using five shear indices (Huesmann and Hitchman 2001). This provides a framework for relating the phase of the QBO to phenomena across a range of levels. The influence of the QBO on the PNJs is shown for each hemisphere, season, and phase of the QBO. In section 5 the effect of midstratospheric QBO wind anomalies on RWB statistics is explored. Then QBO effects in the

tropical stratosphere are contrasted for the middle and upper stratosphere. Conclusions are given in section 6.

2. Data and analysis

The data used in this study are from the National Centers for Environmental Prediction (NCEP) reanalyses (Kalnay et al. 1996; Kistler et al. 2001; www.cdc.noaa.gov), and the 40-yr ECMWF Re-Analysis (ERA-40; Uppala et al. 2005). Because of continuity problems that may have occurred when satellite data first became readily available (Pawson and Fiorino 1998, 1999; Huesmann and Hitchman 2003), only data after 1978 are included in the present study. For NCEP, 27 yr of data (1979–2005) are used; for ECMWF, 24 yr (1979–2002) are used (ending in August 2002). Baldwin and Gray (2005) and Punge and Giorgetta (2006) concluded that ERA-40 represents the QBO with reasonable verisimilitude.

The NCEP reanalyses extend from the surface to 10 hPa, whereas the ECMWF reanalyses extend to 1 hPa. Data are given on a 2.5° grid on pressure levels and interpolated to potential temperature (isentropic) levels. Daily mean PV values were calculated from 6-h means and interpolated to isentropic levels. The daily variability in PV gradient (σ_{P_y}) can be used as a measure of Rossby wave activity.

The RWB statistics are calculated using daily mean PV values as in HH07. For each point, the number of days during which the northward PV gradient is negative ($P_y < 0$; i.e., “reversal days”) is counted. For each reversal, the values of P and P_y are stored. From these data, we calculate reversal frequency (ν , in units of reversal days per 100, or rpc), reversal strength (S , the absolute value of the average gradient on reversal days only), zonal and meridional reversal extent (L_x and L_y), and reversal duration (T).

QBO indices were created for each dataset using the methods of Huesmann and Hitchman (2001). Monthly mean zonal wind anomalies \bar{u}' were defined by subtracting an annual cycle composite. The index for each layer is the upward difference in \bar{u}' at the equator. This index is then used to define each month as characteristically westerly shear (WSh; positive $\partial\bar{u}'/\partial z$), easterly shear (ESh; negative $\partial\bar{u}'/\partial z$), or intermediate. Approximately 1/5 of the months are classified as intermediate, being near the maximum in QBO W or E. There are four indices for NCEP (10–20, 20–30, 30–50, and 50–70) and five for ECMWF (7–10, 10–20, 20–30, 30–50, and 50–70). The relationship between pressure levels and isentropes is shown in Fig. 1. The image breaks at 410 and 850 K emphasize changes in vertical scale. In the tropics these five layers are centered near 900, 800, 700, 550, and

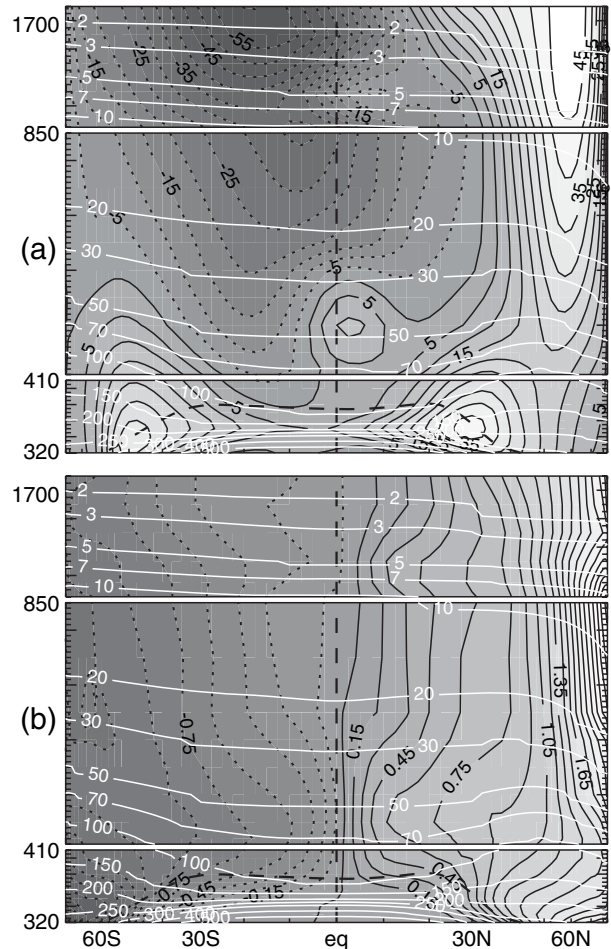


FIG. 1. ERA-40 January 1979 zonal-mean (a) zonal wind (contour interval 5 m s^{-1} ; negative contours dashed) and (b) PV normalized by its global mean profile of the absolute value of PV (contour interval 0.15). Standard pressure levels are shown as white contours.

450 K (Fig. 1). By using lag correlations and these indices, the relationship between a variable and any phase of the QBO can be explored. Results are shown for the December–February (DJF), March–May (MAM), June–August (JJA), and September–November (SON) seasons. For the 24 overlap years, the correlation coefficients between NCEP and ERA-40 shear indices are 0.86 for the 10–20-hPa, 0.89 for the 20–30-hPa, and 0.94 for the 30–50- and 50–70-hPa indices. All of the features emphasized here are apparent in both the NCEP and ERA-40 analyses. ERA-40 results were selected for presenting here.

The statistical significance of relationships between QBO shear indices and other variables was evaluated using Student’s t tests. The score for a difference between two means is compared with expectations from sampling a random population and a statistical significance is

assigned. The 27-yr NCEP record spans about 12 QBO cycles; the 24-yr ECMWF record spans more than 10 cycles. Each season is assumed to be statistically independent from year to year. After subtracting 1/5 of the cases as intermediate, the 27-yr NCEP record contains about 11 independent QBO W–E estimates, and the 24-yr ECMWF record contains about 9 independent QBO W–E estimates for each season. Statistical significance is indicated by shading in QBO W–E difference figures. A QBO W–E difference that is significant at the 97% level means that only three out of 100 sample mean pairs from a random population would have equal or larger differences. Coherence in space and time and consistency with known dynamics are essential for interpreting statistically significant results as causally related.

3. QBO influence on the equatorial PV gradient maximum

ERA-40 zonal-mean winds and PV for January 1979 are shown in Fig. 1. The ERA-40 wind and PV structure agree well with high-vertical resolution Limb Infrared Monitor of the Stratosphere (LIMS) analysis for that month (Hitchman and Leovy 1986). Note the PNJ exceeding 45 m s^{-1} near the stratopause, the summer subtropical westerly jet (SWJ) reaching above 50 hPa near 60°S , and a strong SEJ that extends across the equator in association with the QBO and semiannual oscillation (SAO). QBO W are seen near 50 hPa, overlain by deep QBO E, with a sharp layer of SAO westerly shear near 5 hPa. An examination of the PV contours in Fig. 1b shows that they are pinched together by the convergent QBO meridional flow in W and WSh and spread apart by divergent flow in E and ESh (Hitchman and Leovy 1986). The quantity P_y at the equator is stronger in QBO WSh and weaker in QBO ESh.

The time-mean enhanced PV gradient at the equator reported by HH07 may be due to chronic enhancement at the equator that is modulated by the QBO. The quasi-sinusoidal nature of descending convergence and divergence patterns argues against a nonlinear enhancement by QBO W and a nonzero time mean. An underlying causal agent for the P_y maximum may be that cross-equatorial flow implies inertial instability in the receiving hemisphere, which will tend to create $u_{yy} < 0$ and enhanced P_y at the equator. With stronger negative flow curvature at the equator, one might expect enhanced barotropic instability in the SEJ. The enhanced RWB in the SEJ would tend to “expel” PV contours toward the equator, contributing further to the equatorial P_y maximum.

4. QBO influence on the PNJs

The seasonal cycle in ERA-40 zonal-mean zonal wind provides the context for QBO variations (Fig. 2a). Familiar tropical features include time-mean easterly winds over the equator in the 500–1000-K layer and the SEJs in the spring, summer, and fall. Dunkerton (1989, 1991) showed that this deep layer of time-mean equatorial easterlies and SEJs results from advection of angular momentum by the Brewer–Dobson circulation. In the extratropics the westerly PNJs begin in the fall and end in the spring, with SH flows being much stronger than in the NH. Because planetary Rossby wave activity is stronger in the NH winter than in the SH winter, the NH PNJ experiences more RWB, which decelerates the jet (Fig. 2a). Note the seasonal variation in the SWJs near 350 K and the extension of weak westerlies to $\sim 500 \text{ K}$ over the summer poles. Also significant is the persistent negative curvature in the zonal wind field at the equator in each season: $u_{yy} < 0$, corresponding to the P_y maximum. This feature is also chronic in the NCEP and Met Office analyses (HH07).

QBO WSh–ESh differences in ERA-40 zonal wind for the five indices are shown in Figs. 2b–f. Selecting a different index (and time lag) selects a different stage in the life cycle of the QBO (Huesmann and Hitchman 2001). Some QBO effects can be seen near the subtropical tropopause in some panels, especially in DJF for the 50–70 index and SON for the 7–10 index.

QBO winds affect the PNJ via planetary wave–mean flow interaction, but Fig. 2 suggests that the relationship is complex, with a distinctive Rossby wave structure and flow geometry for each season, hemisphere, and phase of the QBO. The lower left panel confirms the relationship found by Holton and Tan (1980): the NH PNJ is stronger (weaker) during DJF when a QBO W (E) maximum is in the lower stratosphere (Fig. 2f). Let us call this Holton–Tan relationship mode A. This relationship during DJF is also seen in results for the 10–20- and 20–30-hPa shear indices (Figs. 2c,d), although the significance level is less than 90%. This is perhaps due to reduced phase coherence for the lowest stratospheric QBO wind anomaly when the shear index is farther away. There are no significant extratropical signals in the 50–70-hPa index for the NH during MAM, JJA, and SON, and none in the SH (Fig. 2f).

The 20–30- and 30–50-hPa indices (Figs. 2d,e) reveal a significant influence of the QBO on the SH during SON. When a QBO W (E) maximum is in the middle stratosphere (700–800 K or 10–20 hPa), the PNJ in the SH spring is stronger (weaker). This confirms the results reported by Newman and Randel (1988) and Baldwin and Dunkerton (1998). Inspection of Fig. 2e for MAM

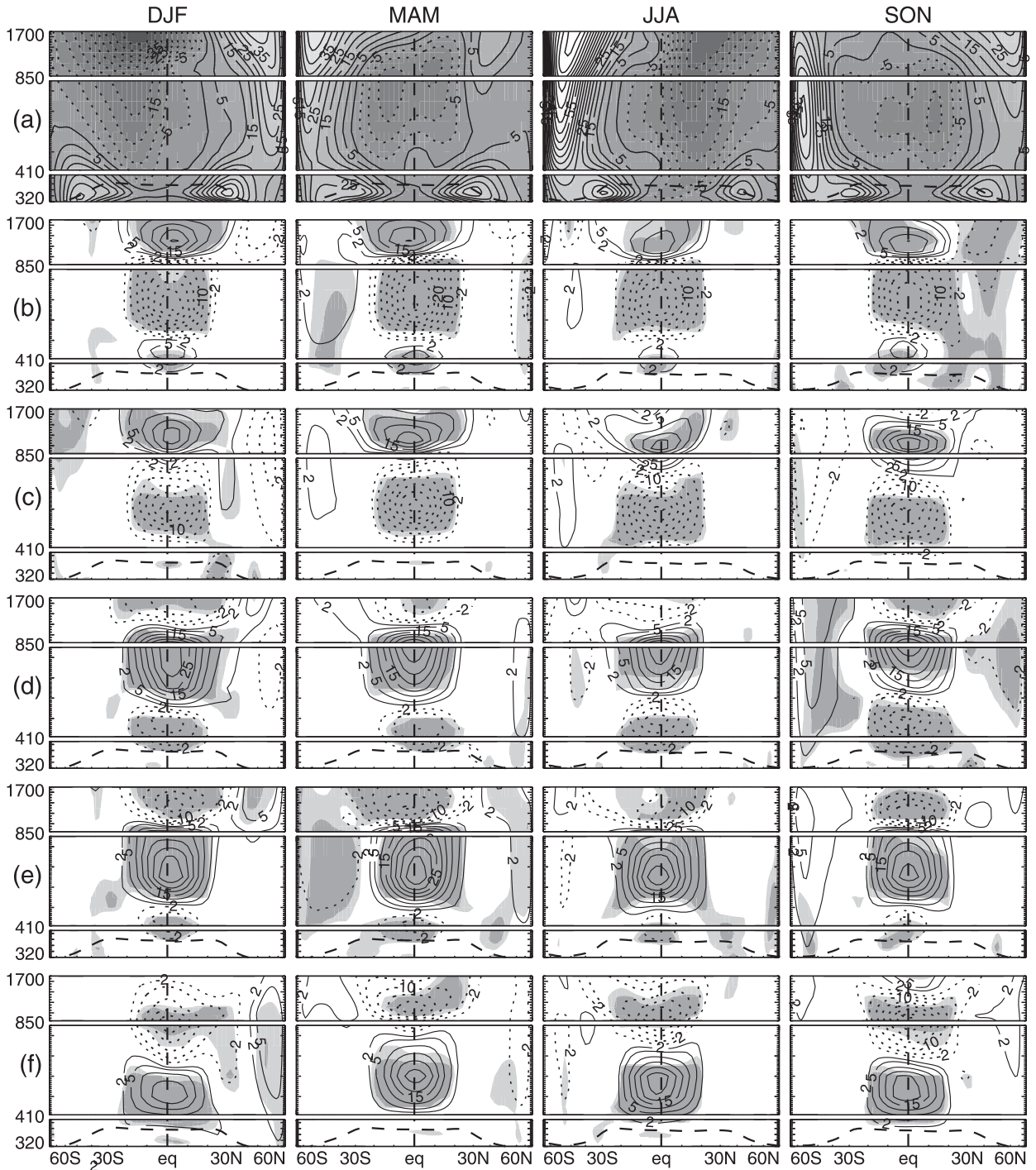


FIG. 2. Seasonally averaged ERA-40 (a) zonal-mean zonal wind (contour interval 5 m s^{-1} ; negative values dashed) and (b)–(f) QBO W – E differences in zonal wind for the (b) 7–10, (c) 10–20, (d) 20–30, (e) 30–50, and (f) 50–70 QBO shear indices (see section 2). In (b)–(f), additional contours are plotted at $\pm 2 \text{ m s}^{-1}$ and the zero contour is omitted. The latitude scale is area equivalent. The tropopause is indicated with a heavy dashed line. Light (dark) shading indicates a significance of 90% (97%).

shows that this relationship also holds for the NH springtime: stronger (weaker) polar winds when a QBO W (E) maximum is in the middle stratosphere. Let us call this mode B. This relationship can also be seen in Fig. 2b for MAM.

Middle-stratospheric QBO wind maxima also affect the PNJs during autumn: a QBO W (E) maximum near 700–800 K coincides with a weaker (stronger) PNJ. Let us call this mode C. The signs of the wind anomalies at low and high latitudes are the same for modes A and B, but are opposite for mode C. The JJA 30–50-hPa index (Fig. 2e) shows a significant influence on the NH summer midlatitude zonal winds near the tropopause. There are also highly significant regions in the mesosphere. These results are consistent with theoretical expectations that QBO wind anomalies alter the critical surfaces for planetary and synoptic waves.

Many studies have explored the effects of the QBO on the NH PNJ. The relationships shown in Fig. 2 provide useful information regarding Rossby wave–mean flow dynamics in other QBO phases and seasons and in the SH. During MAM and SON the wind and Rossby wave structure are different than in DJF, and this is reflected in different relationships between the QBO and the PNJ. Spring and fall seasons usually have narrower and weaker westerly jets and planetary waves are often traveling quickly, especially in the SH. During JJA, the meridionally confined traveling wave-2 interacts with the strong westerly jet in the SH differently than the meridionally more extensive planetary waves in the weaker but broader NH PNJ. These relationships represent points on a continuum envisioned by Fels (1985), with the strong flow, weak wave regime in the SH during JJA and the weak flow, strong wave regime in the NH during DJF representing two of many possible combinations. Differences in NH and SH winter wave regimes are discussed by Shiotani and Hirota (1985).

Seasonal mean and QBO differences in meridional wind are shown in Fig. 3. It should be emphasized that QBO meridional winds are expected to be on the order of 0.2 m s^{-1} ; hence, this variable is less robust than zonal wind. This is reflected in the smaller areas of shading for statistical significance in Fig. 3 relative to Fig. 2. It is also much more affected by dynamical constraints in the assimilation process. The upper panels show the seasonal cycle of meridional wind. During NH winter strong northward flow exists near the stratopause (Fig. 3a, DJF), associated with the boreal winter phase of the SAO (Hitchman and Leovy 1986). There is only a hint of southward flow during austral winter (Fig. 3a, JJA), in agreement with Delisi and Dunkerton (1988), who showed that the “first” SAO cycle is stronger than the “second.” Near the tropical tropopause, northward flow

dominates during DJF and MAM, whereas southward flow dominates during JJA and SON, in agreement with the seasonal change in the Hadley circulation.

The meridional circulation cells associated with the QBO can be seen in Figs. 3b–e. During the solstices (DJF and JJA), QBO E coincide with enhanced flow toward the winter hemisphere, whereas QBO W coincide with reduced flow toward the winter hemisphere. This relationship is consistent with a stronger residual circulation toward the region of enhanced wave activity absorption in the winter hemisphere during QBO E. During the equinoxes (MAM and SON), QBO meridional wind anomalies occur in a quadrupole pattern, with meridional convergence into QBO W. Thus, the solstices are characterized by QBO meridional mass circulation primarily with the winter side, whereas convergence is more symmetric about the equator during the equinoxes. The effects of this on ozone are discussed by Jones et al. (1998).

5. QBO influence on tropical RWB and the SEJs

Previous authors have explored the effects of QBO wind anomalies in the lower stratosphere. Figure 4 explores the effects of middle stratospheric QBO W on tropical jets and RWB statistics using the 30–50-hPa index with zero lag (Fig. 2e). Inspection of Fig. 2 shows that when the 30–50-hPa index is positive, westerlies maximize near 700 K or 20 hPa. Figure 4 shows the zonal-mean distributions of P_y , ν , σ_{P_y} , and S for DJF and JJA, together with the QBO differences in these quantities. An enhanced PV gradient at the equator is seen from the tropopause to the stratopause during both DJF and JJA (Fig. 4a), as shown by HH07. Each PNJ, SEJ, and SWJ is evident in the seasonal mean PV gradient patterns. With QBO W in the middle stratosphere, the PV gradient is enhanced at the equator and diminished in the subtropics (Fig. 4a, columns 2 and 4). The PV gradient anomalies are roughly equal and opposite for QBO E and W; hence, the time-mean PV gradient enhancement is probably not a nonlinear by-product of the QBO itself.

The distributions of ν for DJF and JJA are shown in Fig. 4b (columns 1 and 3). The winter midlatitude surf zones are evident equatorward of the PNJs. The summer polar RWB regime identified by HH07 is also seen. The SEJ on the summer side sports a separate RWB regime. During QBO W and DJF ν is larger in the summer (SH) SEJ (Fig. 4b, column 2), but during QBO W and JJA ν is larger on both sides of the equator (Fig. 4b, column 4).

Variability of the PV gradient is largest in the winter stratosphere and along the tropopause (Fig. 4c, columns 1 and 3), similar to the distribution of planetary and

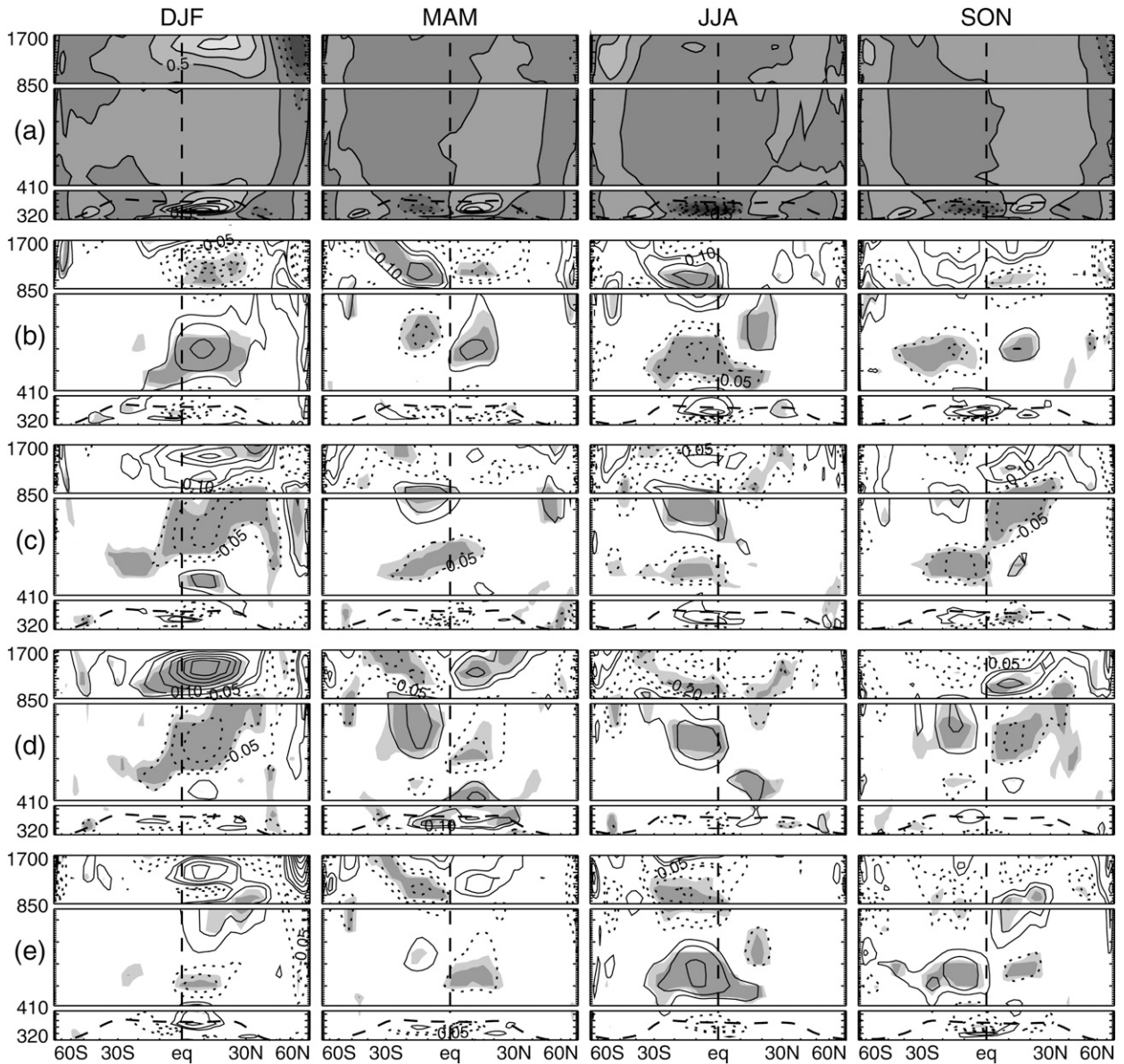


FIG. 3. As in Fig. 2, but for (a) meridional wind (contour interval 0.5 m s^{-1}) and (b)–(e) QBO W – E differences in meridional wind for the (b) 10–20, (c) 20–30, (d) 30–50, and (e) 50–70 QBO shear indices (contour interval 0.05 m s^{-1}).

synoptic Rossby wave activity. With QBO W, during both DJF and JJA there is more penetration of Rossby waves from the winter hemisphere into the tropics, causing greater variability there, with correspondingly less variability in the winter extratropics (Fig. 4c, columns 2 and 4). Above 850 K at this phase of the QBO there is reduced Rossby wave activity in the QBO easterlies in the tropics and enhanced activity in the westerlies over the winter pole.

The solstitial distributions of S are shown in Fig. 4d (columns 1 and 3). RWB is moderately strong in the winter stratosphere and tropopause layer and is espe-

cially strong on the poleward side of the SWJs and PNJs. During QBO W, RWB is stronger at the equator and in the summer SEJ (Fig. 4d, columns 2 and 4). The ν maximum in the winter SH subtropics during JJA (Fig. 4b, column 4) therefore involves quite weak RWB. This supports the idea that QBO W enhances positive curvature and barotropic instability, leading to stronger RWB in the SEJ.

QBO differences in the structure of the PV gradient maximum, SEJs, and associated RWB are compared for the middle and upper stratosphere and for the two solstices in Fig. 5. QBO differences in P_y and ν are shown

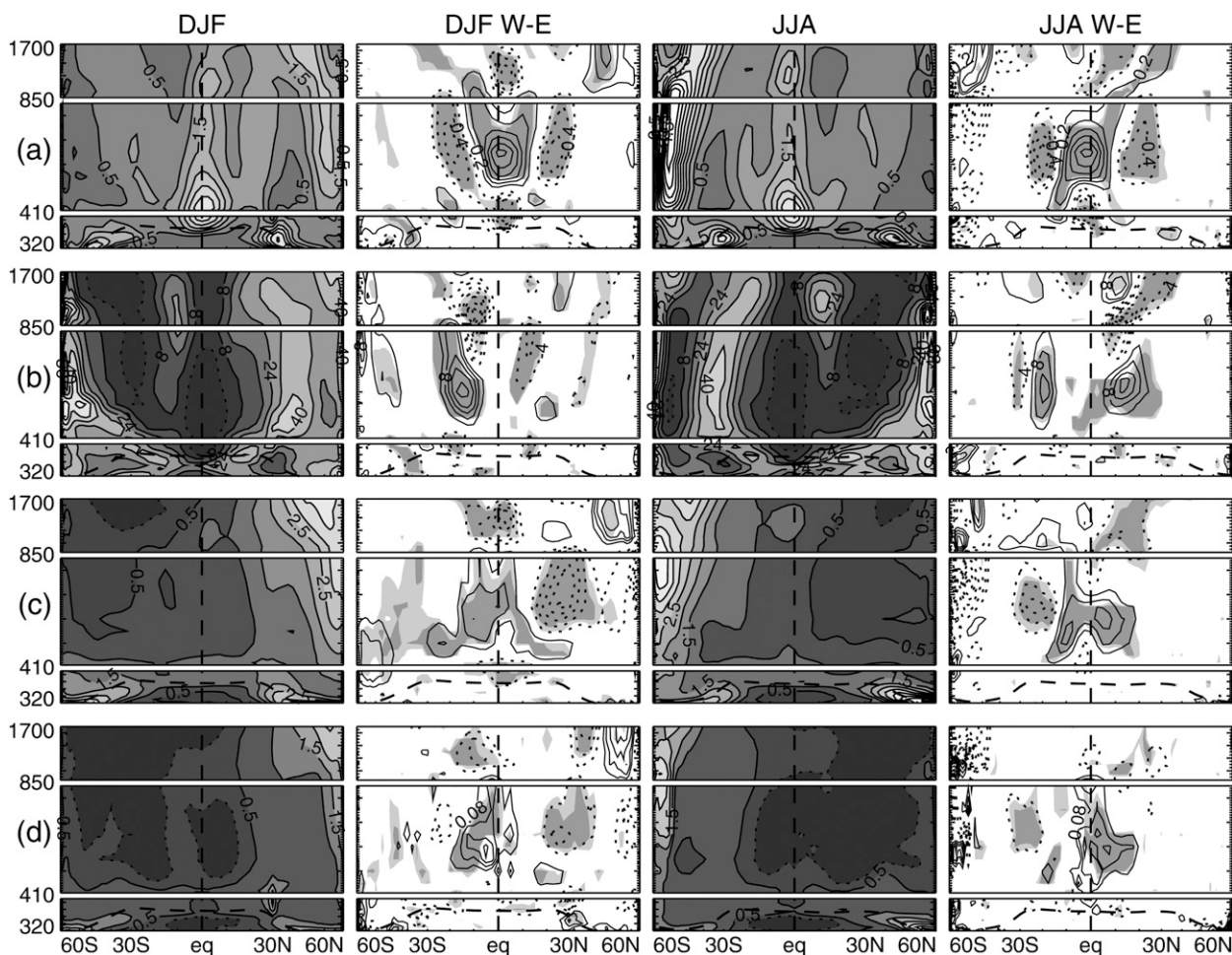


FIG. 4. ERA-40 mean and QBO differences for DJF and JJA using the 30–50 index in (a) P_y , (b) ν , (c) σ_{P_y} , and (d) S . Data in (a), (c), and (d) are scaled by the time and global mean value of P_y at each level. Above 410 K the contour interval in (a), (c), and (d) is 0.5, with an additional contour at 0.3 in (c) and (d). The contour interval in (b) is 8 rpc, with an additional contour at 2 rpc. Below 410 K the contour intervals are smaller: (a) 0.1, (b) 2 rpc, (c) 0.1, and (d) 0.04. In QBO W – E difference plots, light (dark) shading indicates 90% (97%) significance.

at 1300 K using the 7–10-hPa index leading by 2 months (Figs. 5a,b) and at 650 K using the 30–50-hPa index leading by 1 month (Figs. 5c,d). These were selected to give maximum QBO W at each level and to emphasize tropical phenomena. The results for 650 K (Figs. 5c,d) collapse to the zonal-mean values shown in Figs. 4a,b (columns 2 and 4) and correspond to the situation shown in Figs. 2e and 3d (DJF and JJA). The results for 1300 K (Figs. 5a,b) correspond to the situation shown in Fig. 2b (DJF and JJA).

When QBO W are present, the equatorial PV gradient is enhanced. At 650 K this is flanked by subtropical regions of reduced PV gradient (Figs. 5c,d). Shading indicates differences significant above the 85% level, with dark (light) shading indicating a more (less) positive PV gradient during QBO W. In the zonal mean this

relationship is significant at the 97% level (shading in Fig. 4a, columns 2 and 4).

The zonal-mean QBO W–E difference in RWB frequency near 650 K shows more RWB events in the SH subtropics during DJF (Fig. 4b, column 2) but indicates that ν is enhanced in both subtropics during JJA (Fig. 4b, column 4). This is seen in the pattern of circles in Figs. 5c,d. Circle shading is light (dark) for more (fewer) events during QBO W. The statistical significance is shown only for the zonal-mean values (Fig. 4b). At 650 K, light circles are found throughout the SH SEJ during DJF and in both subtropics during JJA, indicating enhanced ν in the SEJ during QBO W. A typical circle size in the subtropics in Fig. 5 is about 10–15 rpc, which agrees with the subtropical maxima in Fig. 4b (columns 2 and 4) for QBO differences. These ranges are

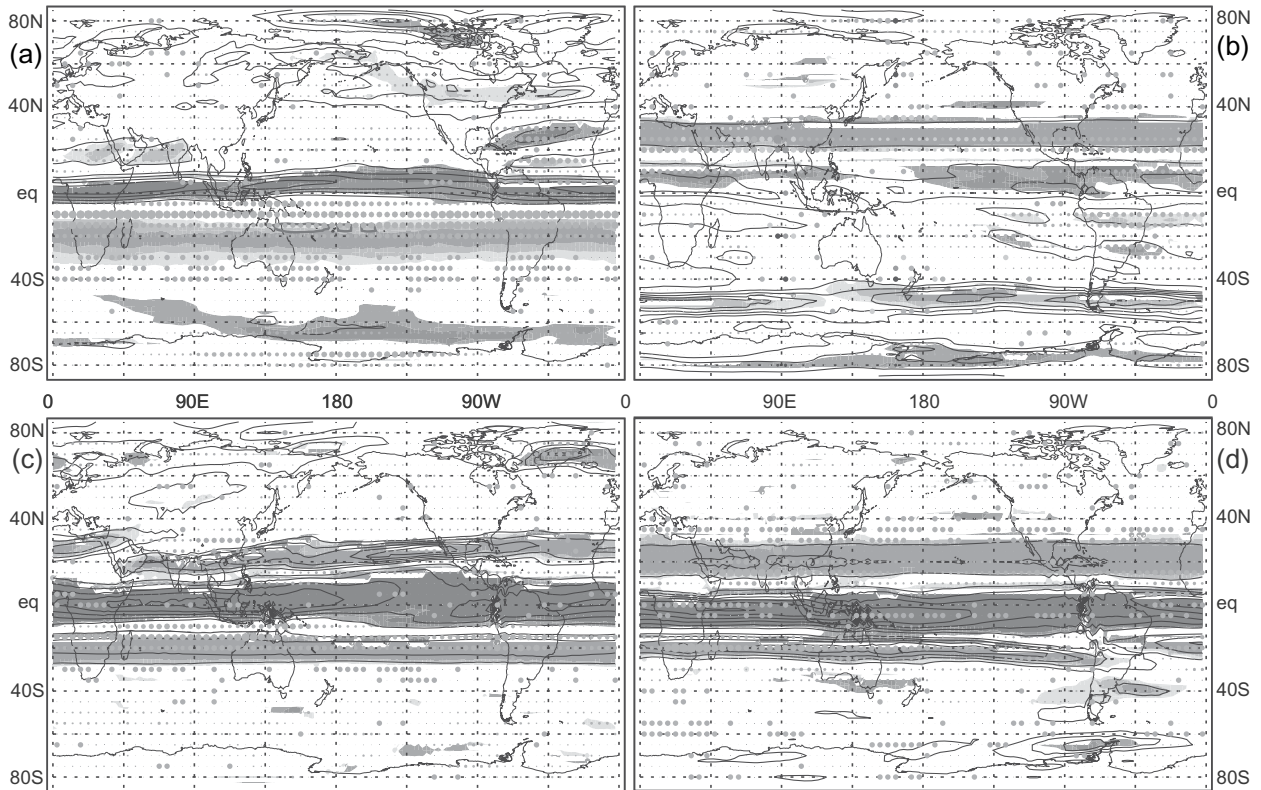


FIG. 5. QBO differences in PV gradient (contours) and RWB frequency (circles) at (a),(b) 1300 K for (a) DJF and (b) JJA (using the 7–10 shear index leading by 2 months) and (c),(d) 650 K for (c) DJF and (d) JJA (using the 30–50 shear index leading by 1 month). The contour interval for W–E differences in PV gradient is 100 PVU per 10° at 1300 K and 6 PVU per 10° at 650 K. Differences exceeding 85% significant are shaded dark (light) for stronger (weaker) PV gradients during QBO W. The circle size indicates W–E differences in RWB frequency (largest = 25 rpe). Circles are shaded light (dark) for more (fewer) RWB events during QBO W. RWB is more frequent on the flanks of QBO W (light circles) where the PV gradient is reduced (light shading).

comparable to the seasonal mean values (Fig. 4b, columns 1 and 3); hence, the QBO exerts a strong influence on RWB frequencies in the tropics.

At 1300 K the equatorial PV gradient is clearly enhanced during QBO W in DJF (Fig. 5a), but less so during JJA (Fig. 5b). In the upper stratosphere flanking negative anomalies occur only on the summer side and they are weaker than at 650 K. QBO differences in RWB frequency at 1300 K show enhancement in the summer SEJ but have no influence on the winter side (Figs. 5a, b). The QBO signal in the PV gradient and the RWB frequency is muted during JJA in the upper stratosphere. This may be related to the much stronger meridional flow from summer to winter hemisphere that exists in the upper stratosphere during DJF (Fig. 3a), the “first” phase of the SAO (Delisi and Dunkerton 1988). In this scenario, stronger inertial instability may erode any chances of in situ wave growth and synoptic RWB on the winter side in the upper stratosphere. During JJA in the upper stratosphere, the weak meridional flow creates a weaker SEJ and weaker inertial in-

stability and RWB. Cross-equatorial flow is weaker in the middle stratosphere (Figs. 5c,d) and the effect of interhemispheric flow is greatly reduced; hence, symmetric enhanced SEJs and RWB exist on both flanks of QBO W.

Throughout Fig. 5 there is a general spatial correlation between light-shaded circles and reduced PV gradient. Where the gradient is less positive (or more negative), there are more RWB events. These regions correspond to a stronger positively curved wind profile or enhanced SEJs with a greater tendency toward instability.

There is a noticeable tendency for QBO W and P_y to be weaker over the central and eastern Pacific and stronger in the Eastern Hemisphere, especially near Indonesia. This may be related to geographical variation in the intensity of convection and associated gravity wave driving. Because the QBO is driven in part by gravity waves illuminating the stratosphere above convection, one might expect westerly gravity waves to drive a more intense local circulation over convection. The narrowness of the arrival of the QBO W regime was studied by Hamilton (1984), Dunkerton and Delisi (1985), and

Hitchman and Leovy (1986), who interpreted it in terms of the convergent meridional circulation at the westerly maximum. Hitchman et al. (1997) suggested that there is a longitudinal preference for this signal in the Indian Ocean–Indonesian sector. Recent work by Hamilton et al. (2004) describes zonal variations in the stratospheric general circulation model and suggests other possible explanations for longitudinal asymmetries in tropical zonal winds. Regionally enhanced inertial instability may play a role, as suggested by potential analogs in the ocean (d’Orgeville et al. 2004; d’Orgeville and Hua 2005). The present climatological results support the existence of this feature reported in previous studies of the tropical middle atmosphere. Further detailed investigation would be required to determine whether this is an artifact of data assimilation or is supported by local observations.

6. Conclusions

Global analyses over 10 QBO cycles were used to explore the influence of the QBO on wind structures and the distribution of RWB. The five shear indices across different layers allowed for a systematic exploration of QBO influence according to QBO phase, season, and hemisphere.

Two previous relationships were confirmed and new statistically significant relationships were described. Primary results may be condensed into the following three modes. Mode A relates lower stratospheric QBO W to a stronger PNJ during NH winter only. Mode B relates middle stratospheric QBO W to a stronger PNJ during spring. Mode C relates middle stratospheric QBO W to a weaker PNJ during fall. The reverse-signed relationship between the QBO and PNJ strength tends to occur for modes A–C when QBO E are present. It would be interesting to carry out idealized simulations to model the wave structure and its interaction with the mean flow for each of these unique combinations.

The effect of the QBO on the equatorial PV gradient maximum was explored. It appears to modulate the equatorial gradient in a quasi-sinusoidal fashion, with distinct enhancement during QBO W. The QBO is probably not the cause of the time-mean maximum, which may result from chronic subtropical RWB associated with inertial and barotropic instabilities.

This study focused on two distinct RWB regimes associated with the PNJs and SEJs. Planetary Rossby waves in the extratropical stratosphere interact significantly with the QBO. They can directly influence the tropics, especially during QBO W. They exist in and modify the PNJ and can influence the extratropical troposphere through vertical coupling. The synoptic-

scale RWB in the subtropics is of a shorter scale and is strongest when the SEJ is most strongly curved.

When QBO W are in the middle stratosphere, the SEJs and RWB are stronger on both sides of the equator. When QBO W are in the upper stratosphere, the SEJ and RWB are enhanced, primarily on the summer side. This effect is strongest during DJF when NH planetary Rossby waves disturb the region and there is a stronger cross-equatorial flow and thus a stronger “first” SAO. Because inertial instability tends to drive flow structure toward smaller and smaller scales (O’Sullivan and Hitchman 1992), realistic simulations of the complex processes associated with this Brewer–Dobson Lagrangian flow would require fairly high resolution.

There is a significant zonal dependence of the equatorial PV gradient maximum and flanking RWB, being stronger in the sector extending from Africa eastward to Indonesia. Gravity wave forcing over convection may intensify local meridional circulations, leading to stronger flow curvatures and increased in situ barotropic instability and RWB. Perhaps future high-resolution observations and simulations can reveal the degree to which these features are real or are artifacts of dynamical data assimilation.

Acknowledgments. The authors were supported by NSF Grant ATM-0342146, NASA ACOMAP Grant NAG5-11303, and a University of Wisconsin—Madison AOS McKinney Fellowship. We thank Warwick Norton, Peter Haynes, Steven Pawson, Ivanka Stajner, and James Anstey for useful conversations and Marek Rogal for help with the figures.

REFERENCES

- Baldwin, M. P., and J. R. Holton, 1988: Climatology of the stratospheric polar vortex and planetary wave breaking. *J. Atmos. Sci.*, **45**, 1123–1142.
- , and T. J. Dunkerton, 1998: Quasi-biennial modulation of the Southern Hemisphere stratospheric polar vortex. *Geophys. Res. Lett.*, **25**, 3343–3346.
- , and —, 2001: Stratospheric harbingers of anomalous weather regimes. *Science*, **294**, 581–584.
- , and Coauthors, 2001: The quasi-biennial oscillation. *Rev. Geophys.*, **39**, 179–229.
- , and L. J. Gray, 2005: Tropical stratospheric zonal winds in ECMWF ERA-40 reanalysis, rocketsonde data, and rawinsonde data. *Geophys. Res. Lett.*, **32**, L09806, doi:10.1029/2004GL022328.
- Berrisford, P., B. J. Hoskins, and E. Tyrlis, 2007: Blocking and Rossby wave breaking on the dynamical tropopause in the Southern Hemisphere. *J. Atmos. Sci.*, **64**, 2881–2898.
- Burkes, D., and C. B. Leovy, 1986: Planetary waves near the mesospheric easterly jet. *Geophys. Res. Lett.*, **13**, 193–196.

- Collimore, C. C., M. H. Hitchman, and D. W. Martin, 1998: Is there a quasi-biennial oscillation in tropical deep convection? *Geophys. Res. Lett.*, **25**, 333–336.
- , D. W. Martin, M. H. Hitchman, A. S. Huesmann, and D. E. Waliser, 2003: On the relationship between the QBO and tropical deep convection. *J. Climate*, **16**, 2552–2568.
- Delisi, D. P., and T. J. Dunkerton, 1988: Seasonal variation of the semiannual oscillation. *J. Atmos. Sci.*, **45**, 2772–2787.
- d'Orgeville, M., and B. L. Hua, 2005: Equatorial inertial-parametric instability of zonally symmetric oscillating shear flows. *J. Fluid Mech.*, **531**, 261–291.
- , R. Schopp, and L. Bunge, 2004: Extended deep equatorial layering as a possible imprint of inertial instability. *Geophys. Res. Lett.*, **31**, L22303, doi:10.1029/2004GL020845.
- Dunkerton, T. J., 1989: Nonlinear Hadley circulation driven by asymmetric differential heating. *J. Atmos. Sci.*, **46**, 956–974.
- , 1991: Nonlinear propagation of zonal winds in an atmosphere with Newtonian cooling and equatorial wave driving. *J. Atmos. Sci.*, **48**, 236–263.
- , and D. P. Delisi, 1985: Climatology of the equatorial lower stratosphere. *J. Atmos. Sci.*, **42**, 376–396.
- Fels, S. B., 1985: Radiative–dynamical interactions in the middle atmosphere. *Advances in Geophysics*, Vol. 28A, Academic Press, 277–300.
- Giorgetta, M. A., L. Bengtsson, and K. Arpe, 1999: An investigation of QBO signals in the east Asian and Indian monsoon in GCM experiments. *Climate Dyn.*, **15**, 435–450.
- Gray, L. J., E. F. Drysdale, T. J. Dunkerton, and B. N. Lawrence, 2001: Model studies of the interannual variability of the Northern Hemisphere stratospheric winter circulation: The role of the quasi-biennial oscillation. *Quart. J. Roy. Meteor. Soc.*, **127**, 1413–1432.
- Gray, W. M., J. D. Sheaffer, and J. A. Knaff, 1990: Influence of the stratospheric QBO on ENSO variability. *J. Meteor. Soc. Japan*, **70**, 975–995.
- Hamilton, K., 1984: Mean wind evolution through the quasi-biennial cycle in the tropical lower stratosphere. *J. Atmos. Sci.*, **41**, 2113–2125.
- , 1998: Effects of an imposed quasi-biennial oscillation in a comprehensive troposphere–stratosphere–mesosphere general circulation model. *J. Atmos. Sci.*, **55**, 2393–2418.
- , A. Hertzog, F. Vial, and G. Stenchikov, 2004: Longitudinal variation of the stratospheric quasi-biennial oscillation. *J. Atmos. Sci.*, **61**, 383–402.
- Hasebe, F., 1983: Interannual variation of global total ozone revealed from Nimbus 4 BUUV and ground-based observations. *J. Geophys. Res.*, **88**, 6819–6834.
- Haynes, P., and E. Shuckburgh, 2000a: Effective diffusivity as a diagnostic of atmospheric transport. 1. Stratosphere. *J. Geophys. Res.*, **105**, 22 777–22 794.
- , and —, 2000b: Effective diffusivity as a diagnostic of atmospheric transport. 2. Troposphere and lower stratosphere. *J. Geophys. Res.*, **105**, 22 795–22 810.
- , C. J. Marks, M. E. McIntyre, T. G. Shepherd, and K. P. Shine, 1991: On the “downward control” of extratropical diabatic circulations by eddy-induced mean zonal forces. *J. Atmos. Sci.*, **48**, 651–678.
- Hitchman, M. H., 1985: An observational study of wave–mean flow interaction in the equatorial middle atmosphere. Ph.D. dissertation, University of Washington, 365 pp.
- , and C. B. Leovy, 1986: Evolution of the zonal mean state in the equatorial middle atmosphere during October 1978–May 1979. *J. Atmos. Sci.*, **43**, 3159–3176.
- , and A. S. Huesmann, 2007: A seasonal climatology of Rossby wave breaking in the 320–2000-K layer. *J. Atmos. Sci.*, **64**, 1922–1940.
- , C. B. Leovy, J. C. Gille, and P. L. Bailey, 1987: Quasi-stationary, zonally asymmetric circulations in the equatorial lower mesosphere. *J. Atmos. Sci.*, **44**, 2219–2236.
- , M. McKay, and C. R. Trepte, 1994: A climatology of stratospheric aerosol. *J. Geophys. Res.*, **99**, 20 689–20 700.
- , and Coauthors, 1997: Mean winds in the tropical stratosphere and mesosphere during January 1993, March 1994, and August 1994. *J. Geophys. Res.*, **102**, 26 033–26 052.
- Holton, J. R., and C.-H. Tan, 1980: The influence of the equatorial quasi-biennial oscillation on the global circulation at 50 mb. *J. Atmos. Sci.*, **37**, 2200–2208.
- , and J. Austin, 1991: The influence of the equatorial QBO on sudden stratospheric warmings. *J. Atmos. Sci.*, **48**, 607–618.
- Huesmann, A. S., and M. H. Hitchman, 2001: The stratospheric quasi-biennial oscillation in the NCEP reanalyses: Climatological structures. *J. Geophys. Res.*, **106**, 11 859–11 874.
- , and —, 2003: The 1978 shift in the NCEP reanalysis stratospheric quasi-biennial oscillation. *Geophys. Res. Lett.*, **30**, 1048, doi:10.1029/2002GL016323.
- Jones, D. B. A., H. R. Schneider, and M. B. McElroy, 1998: Effects of the quasi-biennial oscillation on the zonally averaged transport of tracers. *J. Geophys. Res.*, **103**, 11 235–11 249.
- Kalnay, E., and Coauthors, 1996: The NCEP/NCAR 40-Year Reanalysis Project. *Bull. Amer. Meteor. Soc.*, **77**, 437–471.
- Kinnnersley, J. S., and S. Pawson, 1996: The descent rates of the shear zones of the equatorial QBO. *J. Atmos. Sci.*, **53**, 1937–1949.
- , and K.-K. Tung, 1998: Modeling the global interannual variability of ozone due to the equatorial QBO and to extratropical planetary wave variability. *J. Atmos. Sci.*, **55**, 1417–1428.
- Kistler, R., and Coauthors, 2001: The NCEP–NCAR 50-Year Reanalysis: Monthly means CD-ROM and documentation. *Bull. Amer. Meteor. Soc.*, **82**, 247–267.
- Knox, J. A., and V. L. Harvey, 2005: Global climatology of inertial instability and Rossby wave breaking in the stratosphere. *J. Geophys. Res.*, **110**, D06108, doi:10.1029/2004JD005068.
- Limpasuvan, V., and C. B. Leovy, 1995: Observations of the two-day wave near the southern summer stratopause. *Geophys. Res. Lett.*, **22**, 2385–2388.
- Martius, O., C. Schwierz, and H. C. Davies, 2007: Breaking waves at the tropopause in the wintertime Northern Hemisphere: Climatological analyses of the orientation and theoretical LC1/2 classification. *J. Atmos. Sci.*, **64**, 2576–2592.
- McIntyre, M. E., and T. N. Palmer, 1983: Breaking planetary waves in the stratosphere. *Nature*, **305**, 593–600.
- Naito, Y., M. Taguchi, and S. Yoden, 2003: A parameter sweep experiment on the effects of the equatorial QBO on stratospheric sudden warming events. *J. Atmos. Sci.*, **60**, 1380–1394.
- Nakamura, N., 1996: Two-dimensional mixing, edge formation, and permeability diagnosed in an area coordinate. *J. Atmos. Sci.*, **53**, 1524–1537.
- Newman, P. A., and W. J. Randel, 1988: Coherent ozone–dynamical changes during the Southern Hemisphere spring, 1979–1986. *J. Geophys. Res.*, **93**, 12 585–12 606.
- Niwano, M., and M. Takahashi, 1998: The influence of the equatorial QBO on the Northern Hemisphere winter circulation of a GCM. *J. Meteor. Soc. Japan*, **76**, 453–461.
- Orsolini, Y. J., V. Limpasuvan, and C. B. Leovy, 1997: The tropical stratopause in the UKMO stratospheric analysis: Evidence for

- a 2-day wave and inertial circulations. *Quart. J. Roy. Meteor. Soc.*, **123**, 1707–1724.
- O’Sullivan, D. J., and M. H. Hitchman, 1992: Inertial instability and Rossby wave breaking in a numerical model. *J. Atmos. Sci.*, **49**, 991–1002.
- , and R. E. Young, 1992: Modeling the quasi-biennial oscillation’s effect on the winter stratospheric circulation. *J. Atmos. Sci.*, **49**, 2437–2448.
- , and P. Chen, 1996: Modeling the quasi-biennial oscillation’s influence on isentropic transport in the subtropics. *J. Geophys. Res.*, **101**, 6811–6821.
- Pawson, S., and M. Fiorino, 1998: A comparison of reanalyses in the tropical stratosphere. Part 2: The quasi-biennial oscillation. *Climate Dyn.*, **14**, 645–658.
- , and —, 1999: A comparison of reanalyses in the tropical stratosphere. Part 3: Inclusion of the pre-satellite data era. *Climate Dyn.*, **15**, 241–250.
- Peters, D., and D. W. Waugh, 1996: Influence of barotropic shear on the poleward advection of upper-tropospheric air. *J. Atmos. Sci.*, **53**, 3013–3031.
- , and —, 2003: Rossby wave breaking in the Southern Hemisphere wintertime upper troposphere. *Mon. Wea. Rev.*, **131**, 2623–2634.
- Plumb, R. A., 1983: Baroclinic instability of the summer mesosphere: A mechanism for the quasi-two-day wave? *J. Atmos. Sci.*, **40**, 262–270.
- Postel, G. A., and M. H. Hitchman, 1999: A climatology of Rossby wave breaking along the subtropical tropopause. *J. Atmos. Sci.*, **56**, 359–373.
- , and —, 2001: A case study of Rossby wave breaking along the subtropical tropopause. *Mon. Wea. Rev.*, **129**, 2555–2569.
- Punge, H. J., and M. A. Giorgetta, 2006: Differences between the QBO in the first and in the second half of the ERA-40 reanalysis. *Atmos. Chem. Phys. Discuss.*, **6**, 9259–9271.
- Randel, W. J., and J. B. Cobb, 1994: Coherent variations of monthly mean total ozone and lower stratospheric temperature. *J. Geophys. Res.*, **99**, 5433–5447.
- Reed, R. J., W. J. Campbell, J. A. Rasmussen, and R. G. Rogers, 1961: Evidence of a downward-propagating annual wind reversal in the equatorial stratosphere. *J. Geophys. Res.*, **66**, 613–618.
- Reid, G. C., and K. S. Gage, 1985: Interannual variations in the height of the tropical tropopause. *J. Geophys. Res.*, **90**, 5629–5635.
- Robinson, W. A., 2000: A baroclinic mechanism for the eddy feedback on the zonal index. *J. Atmos. Sci.*, **57**, 415–422.
- Salby, M. L., 1981: Rossby normal modes in nonuniform background configurations. Part II: Equinox and solstice conditions. *J. Atmos. Sci.*, **38**, 1827–1840.
- Semeniuk, K., and T. G. Shepherd, 2001: The middle-atmosphere Hadley circulation and equatorial inertial adjustment. *J. Atmos. Sci.*, **58**, 3077–3096.
- Shiotani, M., 1992: Annual, quasi-biennial, and El Niño–Southern Oscillation (ENSO) time-scale variations in equatorial total ozone. *J. Geophys. Res.*, **97**, 7625–7633.
- , and I. Hirota, 1985: Planetary wave–mean flow interaction in the stratosphere: A comparison between northern and southern hemispheres. *Quart. J. Roy. Meteor. Soc.*, **111**, 309–334.
- Shuckburgh, E., W. Norton, A. Iwi, and P. Haynes, 2001: Influence of the quasi-biennial oscillation on isentropic transport and mixing in the tropics and subtropics. *J. Geophys. Res.*, **106**, 14 327–14 337.
- Thompson, D. W. J., and J. M. Wallace, 2001: Regional climate impacts of the Northern Hemisphere annular mode. *Science*, **293**, 85–89.
- , and S. Solomon, 2002: Interpretation of recent Southern Hemisphere climate change. *Science*, **296**, 895–899.
- , M. P. Baldwin, and S. Solomon, 2005: Stratosphere–troposphere coupling in the Southern Hemisphere. *J. Atmos. Sci.*, **62**, 708–715.
- Trepte, C. R., and M. H. Hitchman, 1992: Tropical stratospheric circulation diagnosed in satellite aerosol data. *Nature*, **355**, 626–628.
- Uppala, S. M., and Coauthors, 2005: The ERA-40 re-analysis. *Quart. J. Roy. Meteor. Soc.*, **131**, 2961–3012.
- Wallace, J. M., 1973: General circulation of the tropical lower stratosphere. *Rev. Geophys. Space Phys.*, **11**, 191–222.
- , and D. W. J. Thompson, 2002: Annular modes and climate prediction. *Phys. Today*, **55**, 28–33.
- Waugh, D. W., and L. M. Polvani, 2000: Climatology of intrusions into the tropical upper troposphere. *Geophys. Res. Lett.*, **27**, 3857–3860.